

## Supporting Information

### **Zn Leaching Reconstructs High-Entropy Hydroxyl Oxides for Efficient Oxygen Evolution Reactions at Large Current Density**

Xiaolong Liang,<sup>a</sup> Ke Xu,<sup>a</sup> Wenqian Qiao,<sup>b</sup> Jing Liang,<sup>a</sup> Tianming Lv,<sup>c</sup> Huanyue  
Zhang,<sup>c</sup> Jun Lu,<sup>a</sup> Lie Zou<sup>a</sup> and Jinxuan Liu<sup>\*a,b</sup>

<sup>a</sup> State Key Laboratory of Fine Chemicals, Dalian University of Technology, 116024  
Dalian, China.

<sup>b</sup> Leicester International Institute, Dalian University of Technology, 116024  
Dalian, China.

<sup>c</sup> Instrumental Analysis Center, Dalian University of Technology, 116024 Dalian,  
China.

\* Jinxuan Liu - State Key Laboratory of Fine Chemicals, Dalian University of  
Technology, 116024 Dalian, China.

E-mail: [jinxuan.liu@dlut.edu.cn](mailto:jinxuan.liu@dlut.edu.cn)

## Experimental Details

### Chemicals and Materials

Potassium hydroxide (KOH, 95%), Nickel nitrate hexahydrate ( $\text{Ni}(\text{NO}_3)_2 \cdot 6\text{H}_2\text{O}$ , 98%), Cobalt (II) nitrate hexahydrate ( $\text{Co}(\text{NO}_3)_2 \cdot 6\text{H}_2\text{O}$ , 99%), Zinc nitrate hexahydrate ( $\text{Zn}(\text{NO}_3)_2 \cdot 6\text{H}_2\text{O}$ , 99%), Iron(III) nitrate nonahydrate ( $\text{Fe}(\text{NO}_3)_3 \cdot 9\text{H}_2\text{O}$ , 98%) were purchased from Macklin. A customized laboratory water purification system was used to purify deionized (DI) water ( $18.2 \text{ } \Omega\text{M} \cdot \text{cm}$  at  $25 \text{ } ^\circ\text{C}$ ). All the above reagents and chemicals were used without further purification in all experiments.

Nickel foam (NF,  $1.5 \text{ mm}$ ,  $250 \text{ g} \cdot \text{m}^{-2}$ ) was purchased from Kunshan Guangjiayuan Co., Ltd., cut into  $2 \times 2.5 \text{ cm}^2$  rectangles, and soaked in  $1 \text{ M HCl}$  solution, acetone, DI water, and absolute ethanol for 15 minutes in an ultrasonic bath, respectively. The cleaned NF was subsequently kept in a vacuum drying oven at  $60 \text{ } ^\circ\text{C}$  for 6 h.

### Synthesis of High-entropy FeCoNiZnOOH/NF catalysts

A conventional three-electrode electrodeposition technique which includes a working electrode (NF), a counter electrode (Pt wire) and a reference electrode (saturated calomel electrode (SCE)) was used to grow FeCoNiZnOOH high-entropy catalyst in-situ on pretreated NF. The electrolyte was prepared by dissolving  $\text{Fe}(\text{NO}_3)_3 \cdot 9\text{H}_2\text{O}$  (0.5 mol),  $\text{Co}(\text{NO}_3)_2 \cdot 6\text{H}_2\text{O}$  (0.5 mol),  $\text{Ni}(\text{NO}_3)_2 \cdot 6\text{H}_2\text{O}$  (0.5 mol), and  $\text{Zn}(\text{NO}_3)_2 \cdot 6\text{H}_2\text{O}$  (0.5 mol) in 50 ml of deionized water (DI). The electrodeposition was carried out at  $-1.0 \text{ V}$  vs. SCE for 30 min. The high-entropy FeCoNiZnOOH/NF electrode was obtained after electrodeposition, then cleaned with deionized water and ethanol, and dried in a vacuum oven at  $60 \text{ } ^\circ\text{C}$  overnight.

For comparison, FeCoNiOOH/NF, FeNiZnOOH/NF, FeCoZnOOH/NF, and CoNiZnOOH/NF were synthesized as comparative materials using a procedure similar to FeCoNiZnOOH/NF, just without  $\text{Zn}(\text{NO}_3)_2 \cdot 6\text{H}_2\text{O}$ ,  $\text{Co}(\text{NO}_3)_2 \cdot 3\text{H}_2\text{O}$ ,  $\text{Ni}(\text{NO}_3)_2 \cdot 6\text{H}_2\text{O}$ , and  $\text{Fe}(\text{NO}_3)_3 \cdot 9\text{H}_2\text{O}$ , respectively.

### Materials Characterization

X-ray diffractometer (XRD, D8 Advance, Germany) with  $\text{CuK}\alpha$  radiation ( $\lambda = 1.5418$

nm, 40 kV, 40 mA) was used to record crystallographic information of the catalyst. Field emission scanning electron microscope (SEM, FEI Nova Nano SEM 450) and transmission electron microscope (TEM, JEM-F200) were used to identify the morphology and map the elemental distribution across the surface of the catalyst. X-ray photon energy spectroscopy (XPS, Axis Supra+) was used to determine the redox state of the sample surface. Raman spectra were recorded using LabRam HR spectrometer (Horiba Jobin Yvon) with a 50X objective microscope. The excitation line was 638 nm with a power of 2.4 mW.

### **Electrocatalytic test**

All the measured potentials vs Hg/HgO were converted to the potential vs reversible hydrogen electrode (RHE) potential ( $E_{RHE} = E_{Hg/HgO} + 0.098V + 0.059pH$ )

### **Cyclic voltammetry (CV) measurements**

CV experiments were performed in 1 M KOH (pH = 13.8) aqueous solution using a three-electrode system connected to an electrochemical workstation (CHI760E, Shanghai, China) at room temperature. Hg/HgO electrode was denoted as the reference electrode and a platinum wire electrode ( $\Phi$ 1 mm) was used as the counter electrode. The working electrodes used for all CV experiments in this work were NF (nickel foam), FeCoNiZnOOH/NF, FeCoNiOOH/NF, FeCoZnOOH/NF, FeNiZnOOH/NF and CoNiZnOOH/NF, respectively.

### **Linear sweep voltammetry (LSV) measurements**

The measurement conditions of LSV are identical to those of CV. The OER activity of the material was measured by LSV with a scan rate of  $5 \text{ mV} \cdot \text{s}^{-1}$  with iR compensation. We used a reverse scan method, from high potential to low potential, to avoid the overlap of oxidation peaks between metal ion and water, which will ensure the accuracy of electrochemical data. The overpotentials ( $\eta$ ) at  $10 \text{ mA} \cdot \text{cm}^{-2}$  were calculated using  $\eta_{10} = E_{RHE} - 1.23 \text{ V}$ . Tafel slopes were calculated using the LSV curves by the Tafel equation:  $\eta = b \log j + a$  where  $\eta$  represents overpotential;  $j$  represents current density;

a is the constant; and b stands for the Tafel slope.

### **Electrochemical active surface area (ECSA) measurements**

CV tests with different scan rates from 20 to 120 mV·s<sup>-1</sup> in the potential range of 0.8 - 0.9 V (vs. RHE) was performed to evaluate the electrochemical active surface area (ECSA) of the electrocatalysts. By plotting the capacitive currents ( $J_{\text{anodic}} - J_{\text{cathodic}}$ ) at 0.85 V (vs. RHE), the double-layer capacitance ( $C_{\text{dl}}$ ) is equal to half of the slope.

### **Stability tests**

Chronopotentiometry (CP) was performed at 100 and 1000 mA·cm<sup>-2</sup> to evaluate the stability of the electrocatalysts without iR correction.

### **In-situ electrochemical Raman experiments**

The experiments were performed in a confocal Raman microscope (LabRam HR, Horiba Yobin Yvon), using a 50X objective. The excitation line was 638 nm from a He-Ne laser with a power of 2.4 mW. Raman spectroscopy was recorded under controlled potentials by an electrochemical workstation. To ensure the accuracy of the test, the parameters are fully consistent with the OER activity tests. It should be emphasized that the electrolytic cell was rectangular, homemade by Teflon and FeCoNiZnOOH/NF was inserted through the wall of the cell to keep the plane of working electrode perpendicular to the incident laser. Each spectrum was acquired within 40 s. All potentials for these experiments were reported versus the reversible hydrogen electrode (RHE) in the working pH (1 M KOH).

### **The configuration entropy ( $S_{\text{config}}$ )**

The configurational entropy was calculated using the following formula.

$$S_{\text{config}} = -R \left[ x \left( \sum_{i=1}^n c_i \ln c_i \right)_{\text{cation-site}} + (1-x) \left( \sum_{j=1}^m c_j \ln c_j \right)_{\text{anion-site}} \right]$$

where  $x$  is the proportion of cation sublattice sites in total equivalent sites and  $1-x$  is equal to the proportion of anion sublattice sites,  $n$ ,  $m$ ,  $c_i$  and  $c_j$  are the total number of

compositional elements for cations, anions, and molar fraction of the  $i$ th element, respectively, and  $R$  is the ideal gas constant ( $8.314 \text{ J mol}^{-1} \text{ K}^{-1}$ ).

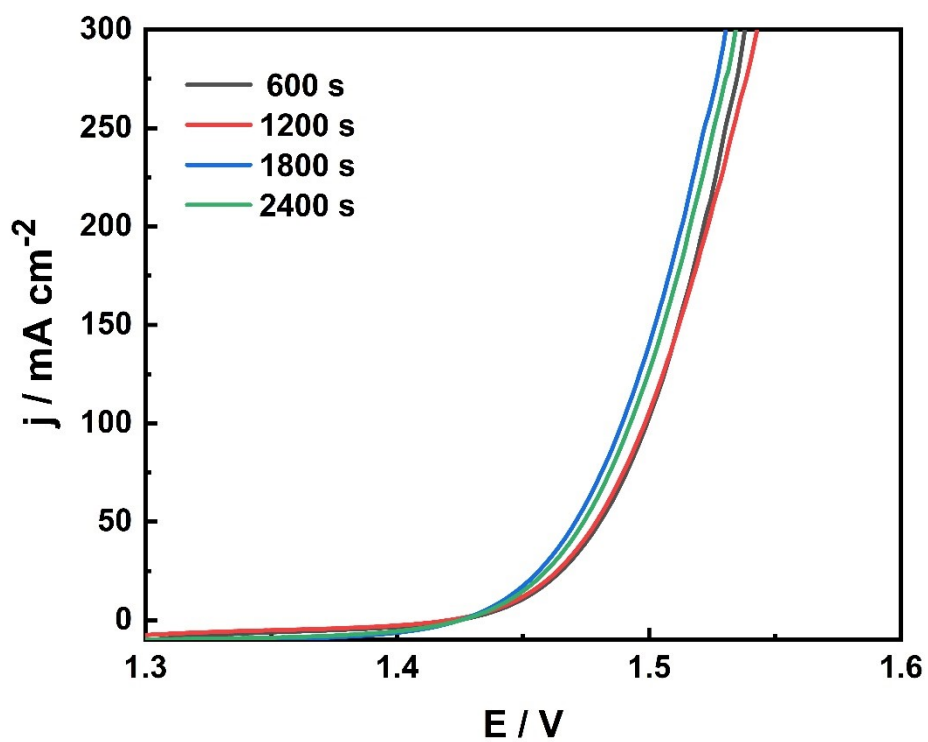


Figure S1 Linear sweep voltammetry curves of high-entropy catalyst with different electrodeposition times.

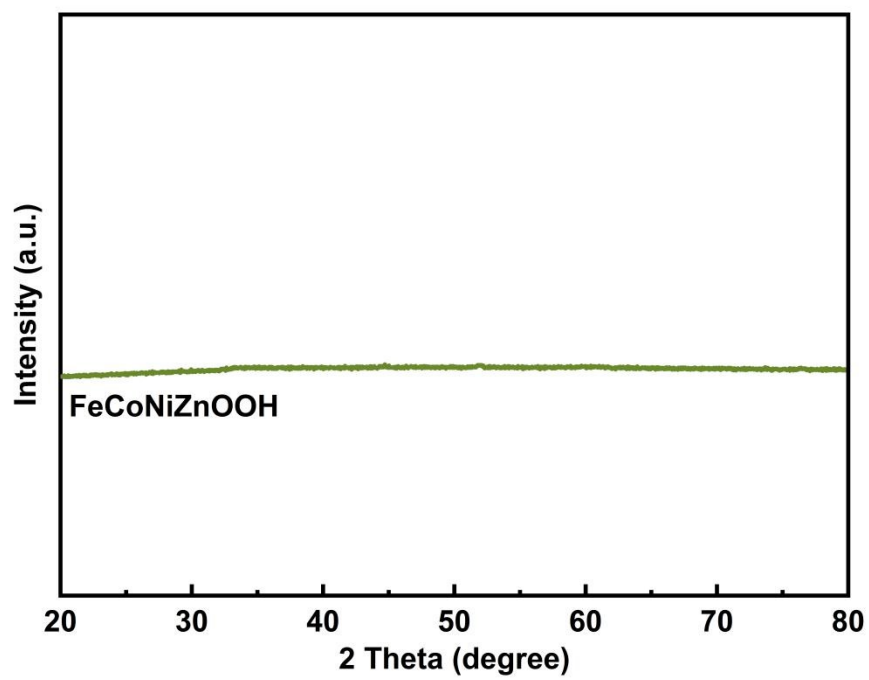


Figure S2 XRD pattern of powder FeCoNiZnOOH.

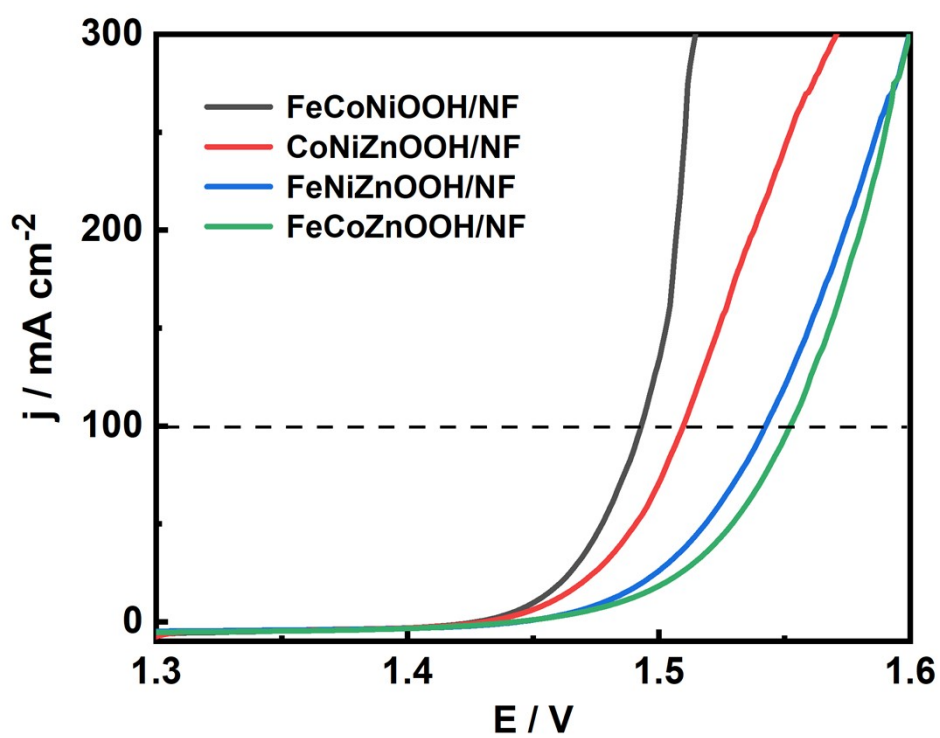


Figure S3 Linear sweep voltammetry curves of FeCoNiOOH/NF, FeCoZnOOH/NF, CoNiZnOOH/NF, and FeNiZnOOH/NF.



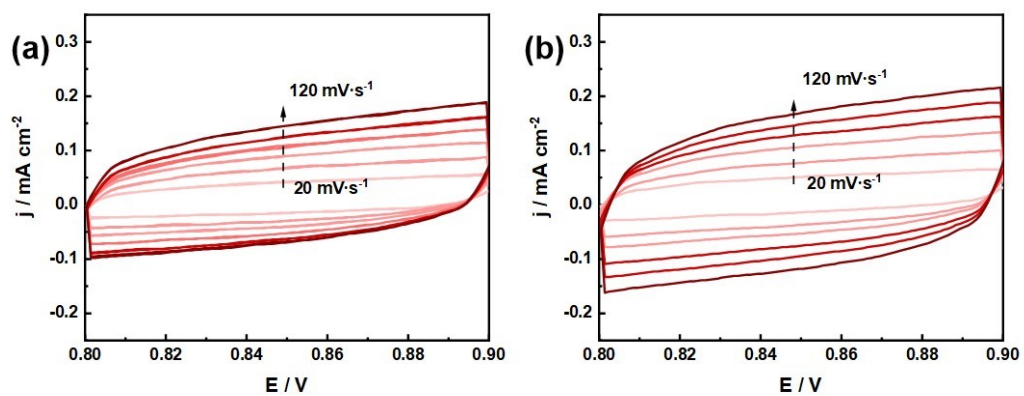


Figure S4 CV curves of (a)  $\text{FeCoNiOOH/NF}$  and (b)  $\text{FeCoNiZnOOH/NF}$  (with varying scan rates: 20, 40, 60, 80, 100 and  $120 \text{ mV}\cdot\text{s}^{-1}$ ) in  $1 \text{ M KOH}$ .

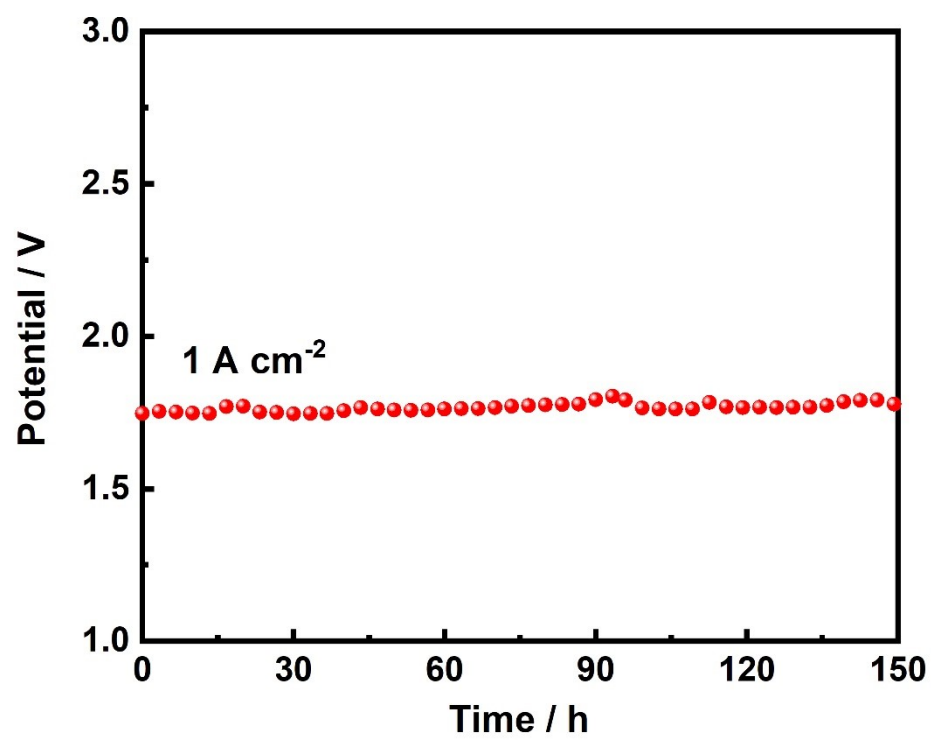


Figure S5 Chronopotentiogram of FeCoNiZnOOH/NF in 1 M KOH at 1 A cm<sup>-2</sup>

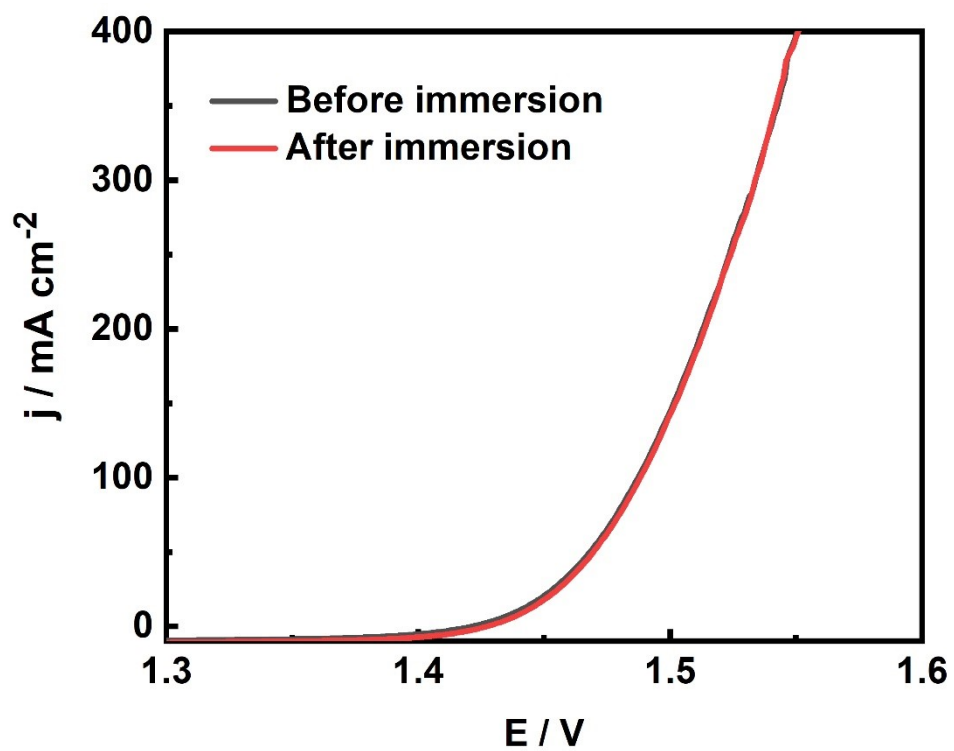


Figure S6 Linear sweep voltammetry curves of FeCoNiZnOOH/NF before and after immersion.

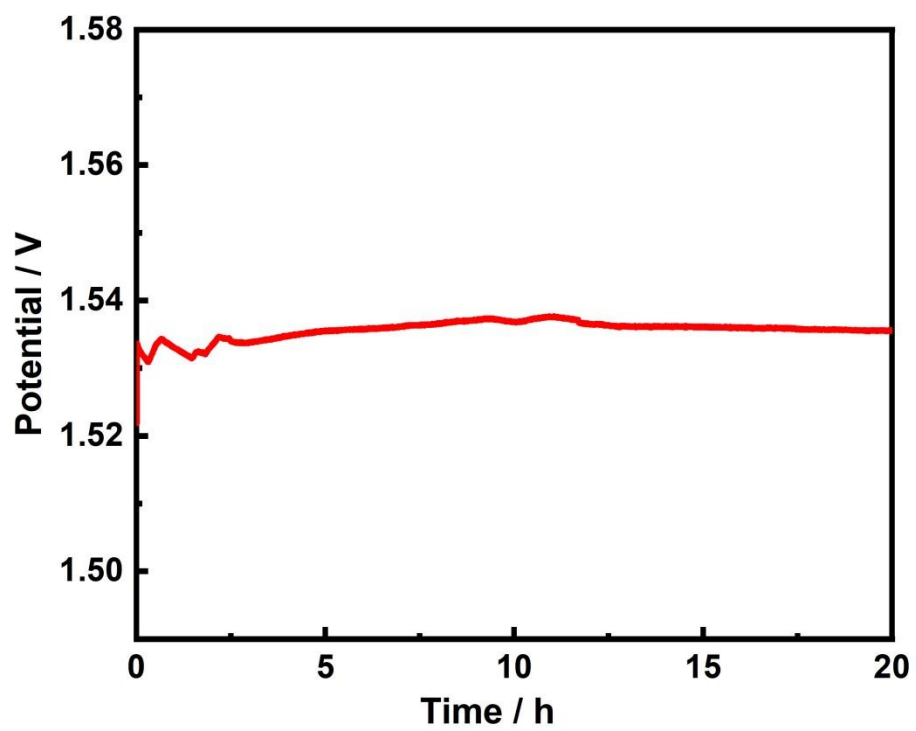


Figure S7 Chronopotentiogram of FeCoNiOOH/NF in 1 M KOH at 100 mA cm<sup>-2</sup>

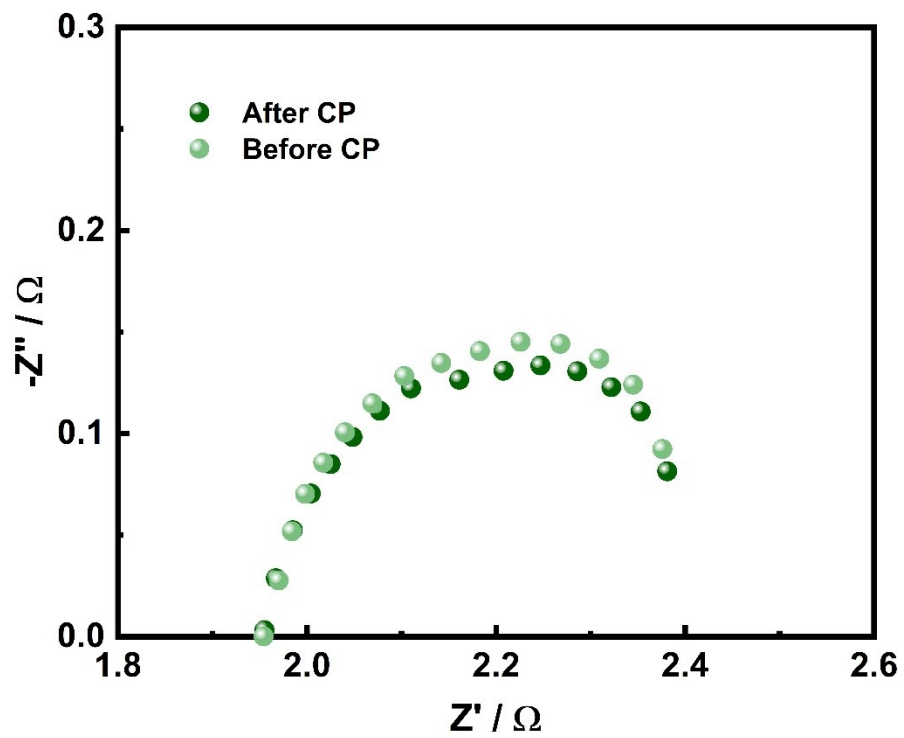


Figure S8 Nyquist plots of FeCoNiZnOOH/NF before and 20 h OER test.

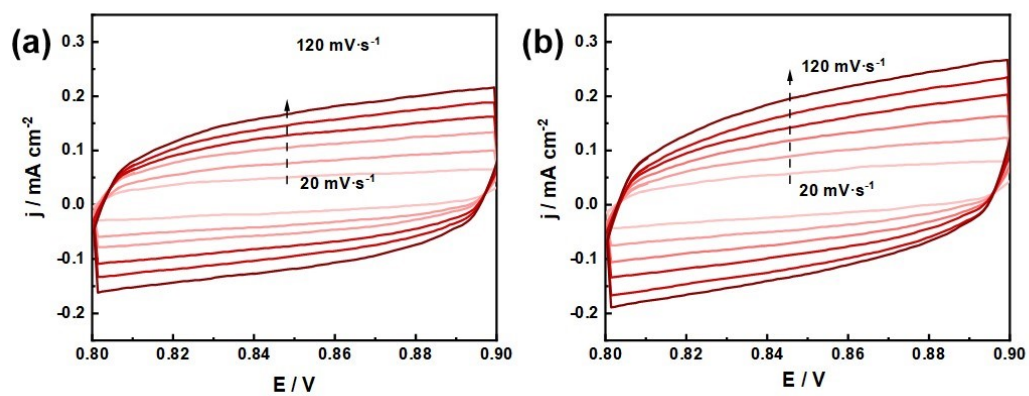


Figure S9 CV curves of FeCoNiZnOOH/NF (a) before and (b) after OER (with varying scan rates: 20, 40, 60, 80, 100 and 120  $\text{mV}\cdot\text{s}^{-1}$ ) in 1 M KOH.

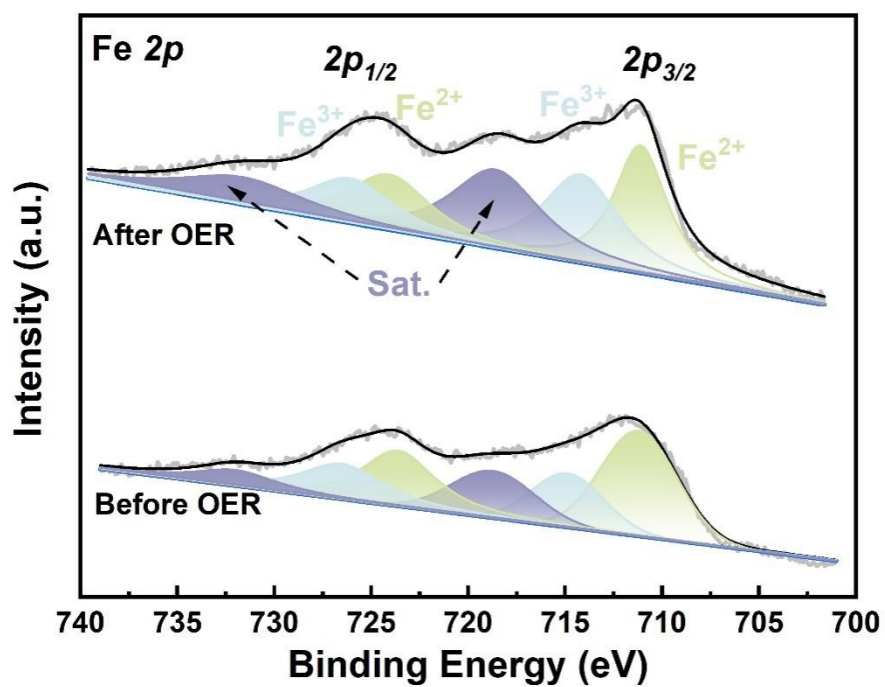


Figure S10 High resolution XPS spectra of Fe 2p for FeCoNiZnOOH/NF catalysts before and after 20 h OER test.

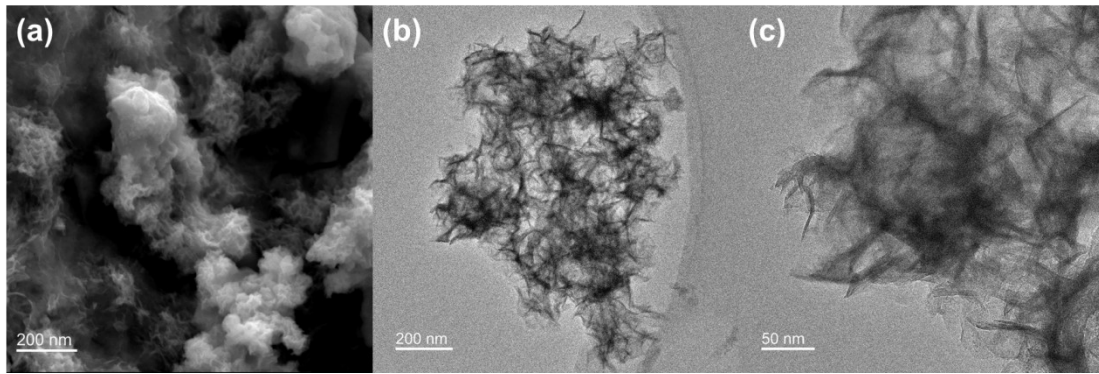


Figure S11 (a) SEM images, (b) and (c) TEM images of the FeCoNiZnOOH/NF catalyst after 20 h OER test.



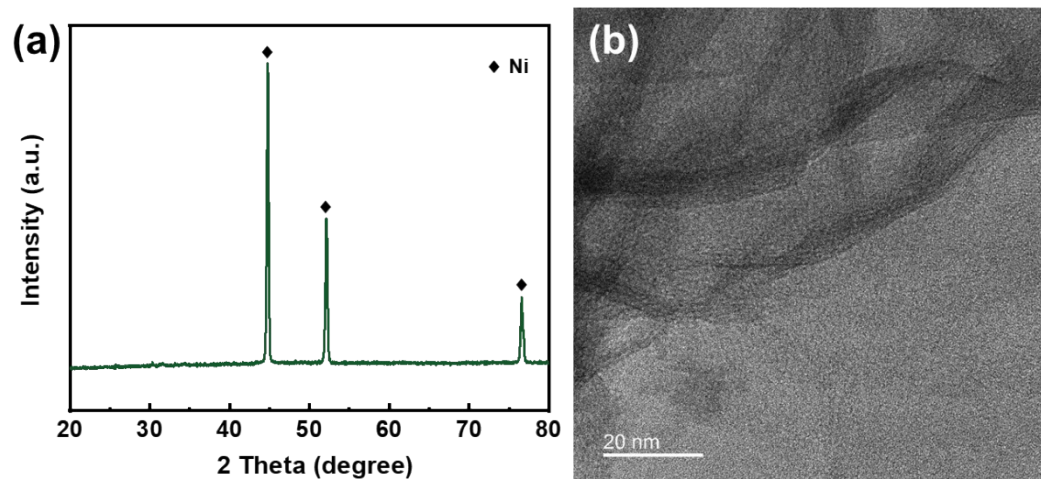


Figure S12 (a) XRD pattern, (b) HRTEM images of the FeCoNiZnOOH/NF catalyst after OER.

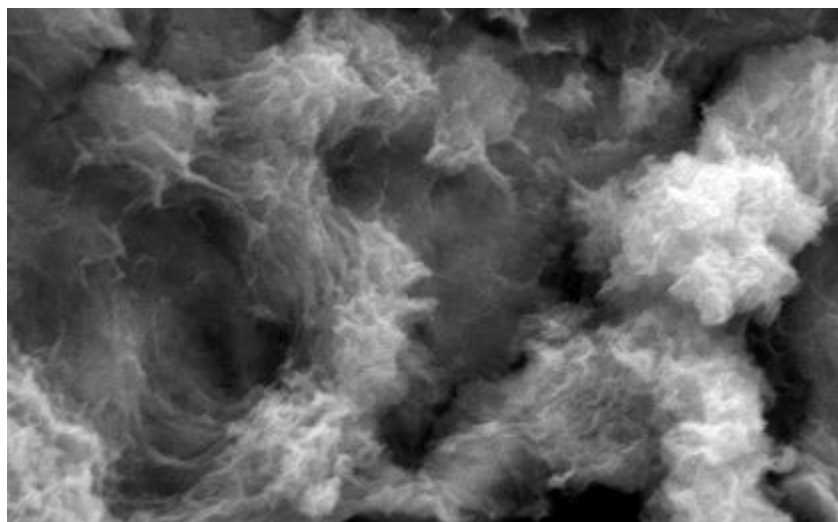


Figure S13 SEM images of the FeCoNiZnOOH/NF catalyst after 150 h OER test.

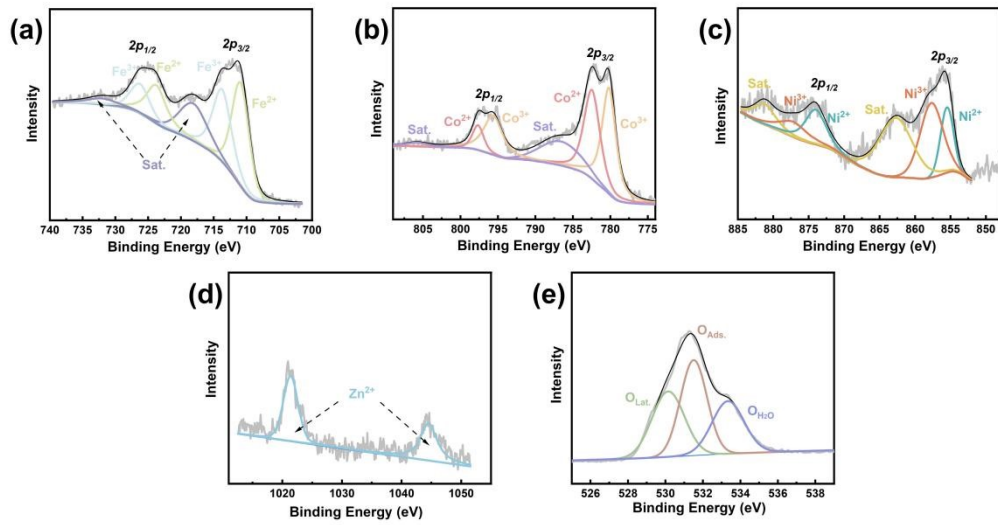


Figure S14 High-resolution XPS spectra of (a) Fe 2p, (b) Co 2p, (c) Ni 2p, (d) Zn 2p  
(e) O1s for FeCoNiZnOOH/NF catalyst after the 150 h OER test.

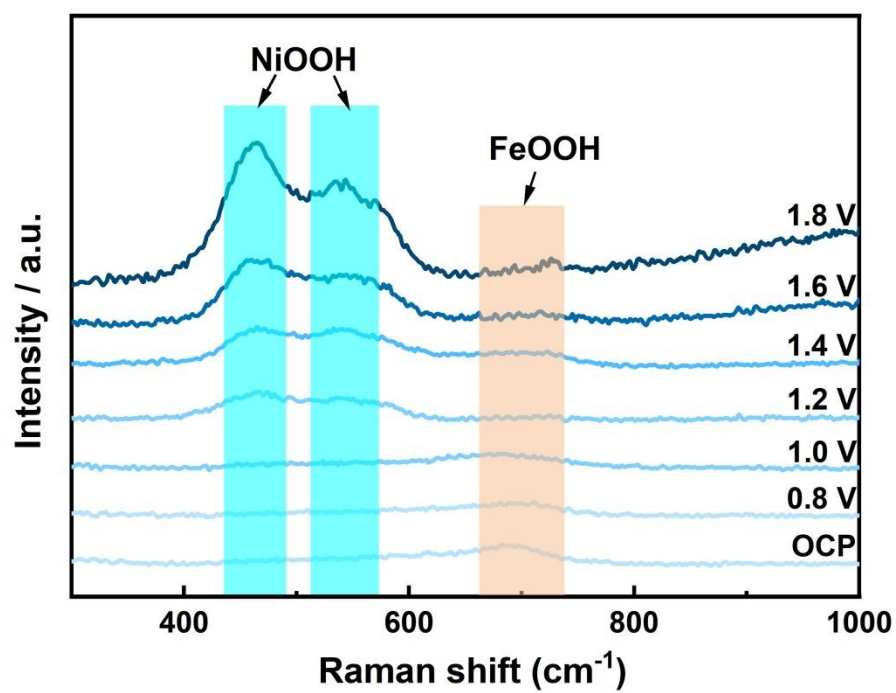


Figure S15 In-situ Raman spectra of FeCoNiOOH for OER in 1 M KOH under different potentials.

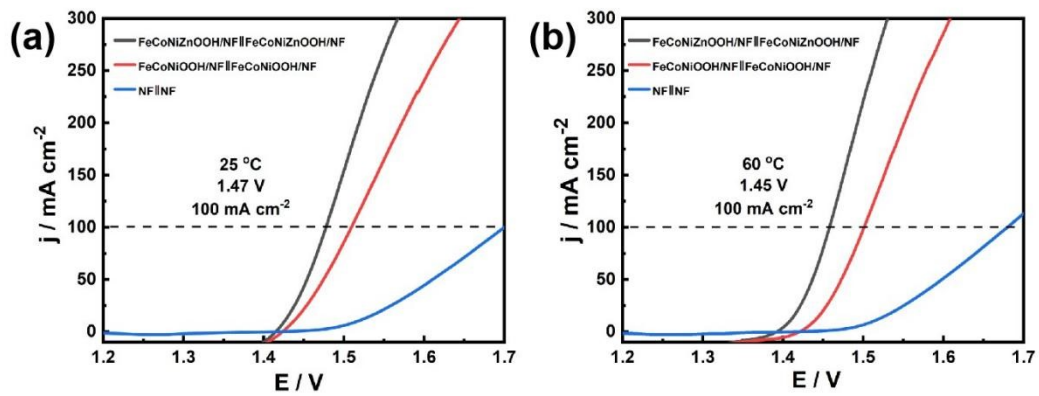


Figure S16 LSV for overall water splitting with the FeCoNiZnOOH/NF electrode as both the anode and cathode in (a) 1 M KOH at 25 °C and (b) 6 M KOH at 60 °C.

Table S1 OER performance for recent typical catalysts in 1 M KOH solution and corresponding references.

Electrocatalysts	Overpotential@ 100 mA/cm <sup>2</sup>	Stability	Electrolyte	Reference
FeCoNiZnOOH/NF	225 mV	150 h	1 M KOH	This work
Fe <sub>3</sub> Co(PO <sub>4</sub> ) <sub>4</sub> @rGO/NF	237 mV	70 h	1 M KOH	[1]
CoCuFeMoOOH	262 mV	72 h	1 M KOH	[2]
Ag@CoCuFeAgMoOOH	270 mV	50 h	1 M KOH	[3]
FeNiCoCrMn-Glycerate	278 mV	36 h	1 M KOH	[4]
NiFeCoMnAl oxide	290 mV	60 h	1 M KOH	[5]
FeCoNiMg-LDH	302 mV	60 h	1 M KOH	[6]
FeCoNiMnRu/CNFs	308 mV	600 h	1 M KOH	[7]
Co <sub>5</sub> Mo <sub>1.0</sub> O NSs@NF	330 mV	140 h	1 M KOH	[8]
np-NiFeCoMnOOH	292 mV	120 h	1 M KOH	[9]
ZnCoNiFeV	259 mV	1000 h	1 M KOH	[10]
FeCoNiMo HEA/C	300 mV	65 h	1 M KOH	[11]

Table S2 Relative proportions of different Fe, Co, Ni and O species before and after the OER.

	$\text{Fe}^{3+}/\text{Fe}^{2+}$	$\text{Co}^{3+}/\text{Co}^{2+}$	$\text{Ni}^{3+}/\text{Ni}^{2+}$	$\text{O}_{\text{lat.}}/\text{O}_{\text{total}}$
Before OER	0.58	0.64	0.68	0.10
After OER	0.63	1.03	1.11	0.48

Table S3 XPS, EDS and ICP results of FeCoNiZnOOH before and after the OER in 1 M KOH.

	Element	XPS (At. %)	EDS (At. %)	ICP (mg/L)
Before OER	Fe	9.5	10.29	7.99
	Co	4.9	5.28	4.32
	Ni	5.5	5.59	--
	Zn	5.8	6.01	9.15
After OER	Fe	10.6	8.95	5.91
	Co	7.6	9.31	6.68
	Ni	8.1	12.39	--
	Zn	1.1	1.03	0.48

*Because nickel foam has a significant impact on ICP test results, the data are not included in the table.*

Table S4 ICP results of 1 M KOH electrolyte before and after the 20 h OER.

Electrolyte	Fe (mg/L)	Co (mg/L)	Ni (mg/L)	Zn (mg/L)
Before OER	0	0	0	0
After OER	0.21	0.02	0.01	1.52



## References

- [1] S. Sultan, M. Ha, D. Y. Kim, J. N. Tiwari, C. W. Myung, A. Meena, T. J. Shin, K. H. Chae and K. S. Kim, *Nat. Commun.* 2019, 10, 5195.
- [2] L. Zhang, W. Cai and N. Bao, *Adv. Mater.* 2021, 33, 2100745.
- [3] L. Zhang, W. Cai, N. Bao and H. Yang, *Adv. Mater.* 2022, 34, 2110511.
- [4] T. X. Nguyen, H. Su, C. Lin, J. Ruan and M. Ting, *Adv. Sci.* 2021, 8, 2002446.
- [5] M. Han, C. Wang, J. Zhong, J. Han, N. Wang, A. Seifitokaldani, Y. Yu, Y. Liu, X. Sun, A. Vomiero and H. Liang, *Appl. Catal., B.* 2022, 301, 120764.
- [6] D. Liu, X. Yan, P. Guo, Y. Yang, Y. He, J. Liu, J. Chen, H. Pan and R. Wu, *ACS Catal.* 2023, 13, 7698-7706.
- [7] J. Hao, Z. Zhuang, K. Cao, G. Gao, C. Wang, F. Lai, S. Lu, P. Ma, W. Dong, T. Liu, M. Du and H. Zhu, *Nat. Commun.* 2022, 13, 2662.
- [8] Y. Zhang, Q. Shao, S. Long and X. Huang, *Nano Energy* 2018, 45, 448.
- [9] Y. Zhang, J. Kang, H. Xie, H. Yin, Z. Zhang, E. Liu, L. Ma, B. Chen, J. Sha, L. Qian, W. Hu, C. He and N. Zhao, *Appl. Catal., B.* 2024, 341, 123331.
- [10] Y. Ding, Z. Wang, Z. Liang, X. Sun, Z. Sun, Y. Zhao, J. Liu, C. Wang, Z. Zeng, L. Fu, M. Zeng and L. Tang, *Adv. Mater.* 2023, 2302860.
- [11] Y. Mei, Y. Feng, C. Zhang, Y. Zhang, Q. Qi and J. Hu, *ACS Catal.* 2022, 12, 17, 10808-10817.